論文 / 著書情報
Article / Book Information

Title	Theoretical derivation of elastic local buckling load formulae of I-shaped steel girders considering web-flange interaction
Authors	Ryohei Kuwada, Kazuya Mitsui
Citation	IABSE Symposium Tokyo 2025
Pub. date	2025, 4

IABSE Symposium 2025
Environmentally Friendly Technologies and Structures - Focusing on Sustainable Approaches
May 18-21, 2025 | Tokyo, Japan

Theoretical derivation of elastic local buckling load formulae of I-shaped steel girders considering web-flange interaction

Ryohei Kuwada

Nippon steel corporation, Futtsu, Japan

Kazuya Mitsui

Institute of Science Tokyo, Meguro, Japan

Contact: kuwada.r6a.ryohhei@jp.nipponsteel.com

Abstract

This study aimed to develop formulae for the elastic critical buckling loads of I-shaped steel girders subjected to uniform bending and pure shear stress by considering the interaction between the web and flange plate elements. The methodology proposed in this study introduces displacement functions that accurately approximate the local buckling deformations of the web and flange in the cross-sections, explicitly formulating the plate–element interaction. Buckling eigenvalue analyses were performed using the finite element method on I-shaped steel girders with various cross-sectional profiles to validate the proposed formulae. By comparing the analysis results with the derived formulae, the proposed formulae were verified to accurately predict the elastic critical local buckling loads.

Keywords: I-shaped girder; elastic critical local buckling; element Interaction; energy method; displacement function; FEM analysis

1 Introduction

In conventional steel structure standards[1]-[3], formulae for each elastic critical buckling load of an I-shaped section member are derived by considering the flange and web as individual plate elements, and various width-to-thickness ratio limits are established based on these formulae. However, when local buckling occurs, the flange and web of an I-shaped section member behave as a unit. Thus, the restraining effect between the plate elements is not considered. Previous studies[4]-[6] have attempted to derive the critical local buckling loads of I-shaped section members composed of multiple plate elements; however, these studies resulted in empirical or regression analysis formulae that do not explicitly formulate the interaction between plate elements. To resolve these problems, in this study, we derive formulae for the elastic critical local buckling loads of I-shaped section members subjected to uniform bending moments and pure shear forces by considering the interaction between the flange and web plate elements. Furthermore, the validity of the formulae was verified through a buckling eigenvalue analysis using the finite element method.

2 Derivation of elastic critical local buckling stress

2.1 Under uniform bending

2.1.1 Proposed displacement function

The buckling analysis target of this section is a local buckling model extracted from an infinitely long I-shaped section member subjected to a uniform bending moment, as shown in Figure 1. In the buckling analysis, the plate thickness was concentrated at the section centerline, and to simplify the calculations, the out-of-plane shear deformation of the plate elements was assumed to be negligible. Additionally, the *x*-*y*-*z* coordinate system shown in Figure 1 was established. The definitions of the parameters and symbols used in Figure 1 and the subsequent derivation process are provided in Table 1.

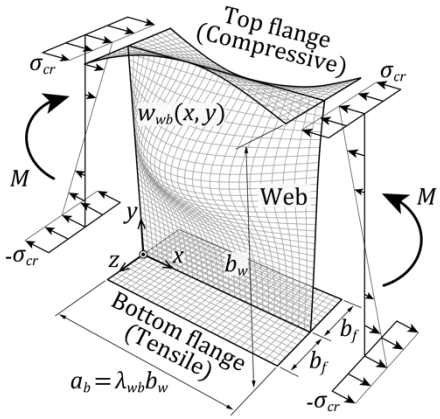

Figure 1. Buckling analysis model under uniform bending

Table 1. Parameters and symbols

H:	Depth [mm]	t_f:	Flange thickness [mm]
B:	Width [mm]	t_w:	Web thickness [mm]
b_w:	H-t_f [mm]	b_f:	B/2 [mm]
Z:	Section modulus [mm^3]	E:	Young's modulus [N/mm^2] (= 205,000)
λ_{wb}:	Web aspect ratio [-] (= a_b/b_w)	v:	Poisson's ratio [-] (= 0.3)
a_b:	Length of half-wave along the x-axis [mm] (= λ_{wb} b_w)		
a_n,b_n:	Undetermined coefficients	σ_{cr}:	Elastic critical local buckling stress [N/mm^2]
D_w:	Flexural rigidity of web plate [N·mm] (= $Et_w^3/[12(1\text{-}v^2)]$)		
D_f:	Flexural rigidity of flange plate [N·mm] (= $Et_f^3/[12(1\text{-}v^2)]$)		

To derive the elastic critical buckling load based on the energy method, the displacement functions of the web and flange must be considered when describing the strain-energy increment in the calculation process. In this study, the buckling deformation of the web half-wavelength was approximated using the partial sum of a finite series, as shown in Eqn. (1).

$$w_{wb} = \sin\frac{\pi x}{a_b}\left\{a_0 + \sum_{n=1}^{N}\left[a_n \cos 2\pi\left(\frac{y}{b_w}\right)^n + b_n \sin\pi\left(\frac{y}{b_w}\right)^n\right]\right\} \quad (1)$$

Notably, the sine functions outside the curly brackets on the right-hand side of Eqn. (1) represent the buckling deformation along the *x*-axis. a_b is the length of the half-wavelength along the *x*-axis and is expressed as the product of the web aspect ratio λ_{wb} and the distance between the centers of the flange thickness b_w, as shown in Table 1. The terms inside the curly brackets on the right-hand side of Eqn. (1) represent the buckling deformation along the *y*-axis of the web and is expressed as a power series of trigonometric functions, where a_n and b_n are the undetermined coefficients of the n^{th} term. Considering the range in which an algebraic solution exists, the displacement function along the *y*-axis of the web is approximated using Eqn. (2), which uses the partial sum of Eqn. (1).

$$w_{wb} = \sin\frac{\pi x}{a_b}\left[\alpha_b \sin\frac{\pi y^2}{b_w} + \beta_b\left(1 - \cos\frac{2\pi y^2}{b_w}\right)\right] \quad (2)$$
$$\left(N = 2, \alpha_b = b_2, \beta_b = a_0 = -a_2, a_1 = b_1 = 0\right)$$

Then, using the displacement function of the web from Eqn. (2), the displacement function of the flange was determined. The center of rotation of the flange was assumed to be the junction line between the web and flanges, and it was assumed that the flange deformed out-of-plane while remaining straight and perpendicular to the web. The displacement functions of the top and bottom flanges can be derived by substituting $y = b_w$ and $y = 0$ into Eqn. (3), which was obtained by partially differentiating Eqn. (2) with respect to *y*, which results in Eqns. (4-5).

$$\frac{\partial w_{wb}}{\partial y} = -\frac{2\pi}{b_w^2}\sin\frac{\pi x}{a_b}\left[\alpha_b y \cos\frac{\pi y^2}{b_w} + 2\beta_b y \sin\frac{2\pi y^2}{b_w}\right] \quad (3)$$

$$\text{Top flange: } w_{ftb} = z \cdot \left.\frac{\partial w_w}{\partial y}\right|_{y=b_w} = -\frac{\pi\alpha}{b_w} z \sin\frac{\pi x}{a_b} \quad (4)$$

$$\text{Bottom flange: } w_{fbb} = z \cdot \left.\frac{\partial w_w}{\partial y}\right|_{y=0} = 0 \tag{5}$$

2.1.2 Derivation of buckling stress formula

In this subsection, a formula for the elastic critical buckling load of I-shaped section members subjected to a uniform bending moment is derived based on the energy method. Assuming the bending stresses acting on the flange and web of the I-shaped section member at the elastic critical buckling load, as shown in Figure 1, the increments of external potential energy for the web, top flange, and bottom flange, denoted as ΔV_{wb}, ΔV_{ftb}, and ΔV_{fbb}, can be described using Eqns. (6-8).

$$\Delta V_{wb} = -\int_0^{b_w} \sigma_{cr} t_w \delta_b \left(\frac{2y}{b_w} - 1\right)^2 dy \tag{6}$$

$$\Delta V_{ftb} = -\int_{-b_f}^{b_f} \sigma_{cr} t_f \delta_b dz \tag{7}$$

$$\Delta V_{fbb} = -\int_{-b_f}^{b_f} \sigma_{cr} t_f \delta_b dz\ , \tag{8}$$

where δ_b is the small displacement of the flange caused by the external force. Additionally, the increments of strain energy for the web, top flange, and bottom flange, denoted as ΔU_{wb}, ΔU_{ftb}, and ΔU_{fbb}, can be described using Eqns. (9-11), considering the compatibility conditions of the axial displacements caused by the out-of-plane deformation of each plate element.

$$\begin{aligned}\Delta U_{wb} = {} & \frac{D_w}{2}\int_0^{a_b}\int_0^{b_w}\left[\left(\frac{\partial^2 w_{wb}}{\partial x^2}\right)^2 + \left(\frac{\partial^2 w_{wb}}{\partial y^2}\right)^2\right. \\ & \left. +2\nu\left(\frac{\partial^2 w_{wb}}{\partial x^2}\right)\left(\frac{\partial^2 w_{wb}}{\partial y^2}\right) + 2(1-\nu)\left(\frac{\partial^2 w_{wb}}{\partial x \partial y}\right)^2\right] dydx \\ & + \int_0^{a_b}\int_0^{b_w} \sigma_{cr}\left(\frac{2y}{b_w} - 1\right) t_w \cdot \left[\frac{\delta_b}{a}\left(\frac{2y}{b_w} - 1\right) - \frac{1}{2}\left(\frac{\partial w_{wb}}{\partial x}\right)^2\right] dydx\end{aligned} \tag{9}$$

$$\begin{aligned}\Delta U_{ftb} = {} & \frac{D_f}{2}\int_0^{a_b}\int_{-b_f}^{b_f}\left[\left(\frac{\partial^2 w_{ftb}}{\partial x^2}\right)^2 + \left(\frac{\partial^2 w_{ftb}}{\partial z^2}\right)^2\right. \\ & \left. +2\nu\left(\frac{\partial^2 w_{ftb}}{\partial x^2}\right)\left(\frac{\partial^2 w_{ftb}}{\partial z^2}\right) + 2(1-\nu)\left(\frac{\partial^2 w_{ftb}}{\partial x \partial z}\right)^2\right] dzdx \\ & + \int_0^{a_b}\int_{-b_f}^{b_f} \sigma_{cr} t_f \left[\frac{\delta_b}{a} - \frac{1}{2}\left(\frac{\partial w_{ftb}}{\partial x}\right)^2\right] dzdx\end{aligned} \tag{10}$$

$$\begin{aligned}\Delta U_{fbb} = {} & \frac{D_f}{2}\int_0^{a_b}\int_{-b_f}^{b_f}\left[\left(\frac{\partial^2 w_{fbb}}{\partial x^2}\right)^2 + \left(\frac{\partial^2 w_{fbb}}{\partial z^2}\right)^2\right. \\ & \left. +2\nu\left(\frac{\partial^2 w_{fbb}}{\partial x^2}\right)\left(\frac{\partial^2 w_{fbb}}{\partial z^2}\right) + 2(1-\nu)\left(\frac{\partial^2 w_{fbb}}{\partial x \partial z}\right)^2\right] dzdx \\ & + \int_0^{a_b}\int_{-b_f}^{b_f} \sigma_{cr} t_f \left[\frac{\delta_b}{a} - \frac{1}{2}\left(\frac{\partial w_{fbb}}{\partial x}\right)^2\right] dzdx\end{aligned} \tag{11}$$

Based on these equations, the total potential energy increment $\Delta\Pi_b$, which is represented by the sum of the strain energy increments and the external potential energy increments, can be obtained as shown in Eqn. (12).

$$\Delta\Pi_b = \Delta U_{wb} + \Delta U_{ftb} + \Delta U_{fbb} + \Delta V_{wb} + \Delta V_{ftb} + \Delta V_{fbb} \tag{12}$$

From the stationary condition of the total potential energy, the first variations of Eqn. (12) with respect to the coefficients α_b and β_b yield Eqns. (13-14).

$$\frac{\partial \Delta\Pi_b}{\partial \alpha_b} = 0 \tag{13}$$

$$\frac{\partial \Delta\Pi_b}{\partial \beta_b} = 0 \tag{14}$$

After performing these differentiations and simplifying them, the buckling condition equation can be obtained as shown in Eqn. (15).

$$\begin{Bmatrix} m_1 - m_2\sigma_{cr} & m_3 - m_4\sigma_{cr} \\ m_3 - m_4\sigma_{cr} & m_5 - m_6\sigma_{cr} \end{Bmatrix} \begin{pmatrix} \alpha_b \\ \beta_b \end{pmatrix} = 0 \tag{15}$$

Local buckling occurred when Eqn. (15) provides a solution other than the trivial solution ($\alpha_b = \beta_b = 0$). Consequently, the determinants of the coefficient matrix on the left-hand side of Eqn. (15) must be zero. Therefore, by calculating the conditions under which the determinant of the coefficient matrix is zero, Eqn. (16) can be obtained.

$$\begin{aligned}&\left(m_2 m_6 - m_4^2\right)\sigma_{cr}^2 - \left(m_1 m_6 + m_2 m_5 - 2m_3 m_4\right)\sigma_{cr} \\ &+ m_1 m_5 - m_3^2 = 0\end{aligned} \tag{16}$$

As Eqn. (16) is a quadratic equation with respect to the critical buckling stress σ_{cr}, it should be noted that the minimum positive value of the obtained solutions is the actual critical buckling stress. Consequently, σ_{cr} can be obtained as shown in Eqn. (17).

$$\sigma_{cr} = \frac{B_b - \sqrt{B_b^2 - 4A_b C_b}}{2A_b} \tag{17}$$

$$A_b = m_2 m_6 - m_4^2 \tag{17a}$$

$$B_b = m_1 m_6 + m_2 m_5 - 2m_3 m_4 \tag{17b}$$

$$C_b = m_1 m_5 - m_3^2\ , \tag{17c}$$

where m_1–m_6 are functions of λ_{wb}, as shown in Eqns. (18-23).

$$m_1 = \frac{D_w}{2b_w^2}\left\{\frac{\pi^2}{2\lambda_{wb}^2}(1-C_1)+4\pi^2\left[(1-2\nu)C_3-\frac{\nu}{2\pi}S_2+\frac{1}{3}\right]\right.$$
$$+2\lambda_{wb}^2\left[1+C_1+\frac{4\pi^2}{5}(1-5C_2)-4\pi S_1\right] \quad (18)$$
$$\left.+\frac{8\pi^2 D_f b_f}{D_w b_w}\left[\frac{\pi^2 b_f^2}{3\lambda_{wb}^2 b_w^2}+2(1-\nu)\right]\right\}$$

$$m_2 = t_w\left(\frac{C_1}{4}+\frac{4\pi^2 b_f^3 t_f}{3b_w^3 t_w}\right) \quad (19)$$

$$m_3 = \frac{D_w}{2b_w^2}\left\{\frac{\pi^2}{2\lambda_{wb}^2}(3S_3-S_4)+4\lambda_{wb}^2\left[2\pi(C_4+3C_5)+S_3\right.\right.$$
$$\left.+S_4+8\pi^2(S_5-S_6)\right]-3\pi\nu(C_6-C_7) \quad (20)$$
$$\left.+2\pi^2\left[(3\nu+4)S_7-(9\nu-4)S_8\right]\right\}$$

$$m_4 = t_w\left[\frac{4}{3\pi}-\frac{1}{4}(3S_3-S_4)\right] \quad (21)$$

$$m_5 = \frac{D_w}{2b_w^2}\left\{\frac{\pi^2}{2\lambda_{wb}^2}(3-4C_1+C_8)\right.$$
$$+8\lambda_{wb}^2\left[1-C_8+\frac{16\pi^2}{5}(1+5C_9)+8\pi S_9\right] \quad (22)$$
$$\left.+\frac{16\pi^2}{3}\left[1-6\nu C_3-3(1-2\nu)C_{10}\right]-4\pi\nu(2S_2-S_{10})\right\}$$

$$m_6 = t_w\left(C_1-\frac{C_8}{4}\right), \quad (23)$$

where C_1–C_{10} and S_1–S_{10} are definite integral terms as shown in Appendix A. The critical local buckling stress σ_{cr} needs to be minimized with respect to λ_{wb} in Eqn. (17). In other words, by calculating λ_{wb} that satisfies Eqn. (24), the critical local buckling stress σ_{cr} can be obtained.

$$\frac{\partial \sigma_{cr}}{\partial \lambda_{wb}} = 0 \quad (24)$$

The accuracy of the predicted elastic critical buckling stress σ_{cr} that satisfies Eqn. (24) was verified by comparing it with the results of the buckling eigenvalue analysis using the finite element method, as described in Section 3:

2.2 Under pure shear force

2.2.1 Proposed displacement function

The buckling analysis target in this section was a shear buckling model extracted from an infinitely long I-shaped section member subjected to a pure shear force on the web, as shown in Figure 2. The assumptions for the buckling analysis are the same as those in the previous section. Additionally, the *x*-*y*-*z* coordinate system was redefined. The definitions of the parameters and symbols used in Figure 2 and the subsequent derivation process are provided in Table 2. The parameters and symbols are not listed in Table 1. In this section, the buckling deformation of the half-wavelength of the web, which experiences a phase shift in the *y*-axis, as shown in Figure 2, is approximated by the partial sum of the finite series shown in Eqn. (25).

$$w_{ws} = \sin\left[\frac{\pi}{a_s}\left(x+\xi b_w \sin\frac{\pi y}{b_w}\right)\right]$$
$$\cdot\left\{c_0+\sum_{n=1}^{N}\left[c_n\cos\pi\left(\frac{2y}{b_w}\right)^n+d_n\cos\frac{\pi}{2}\left(\frac{2y}{b_w}\right)^n\right]\right\} \quad (25)$$

The sine functions outside the curly brackets on the right-hand side of Eqn. (25) represent the buckling deformation along the *x*-axis, and the second term inside the parentheses of the sine function represents the phase shift along the *y*-axis, with ξ being the coefficient that determines the magnitude of phase shift. The parameter a_s is the length of the half-wavelength along the *x*-axis and is expressed as the product of the web aspect ratio λ_{ws} and the distance between the centers of the flange thickness b_w, as shown in Table 2. The terms inside the curly brackets on the right-hand side of Eqn. (25) represent the buckling deformation along the *y*-axis of the web, which is expressed as a power series of trigonometric functions, where c_n and d_n are the undetermined coefficients of the n^{th} term.

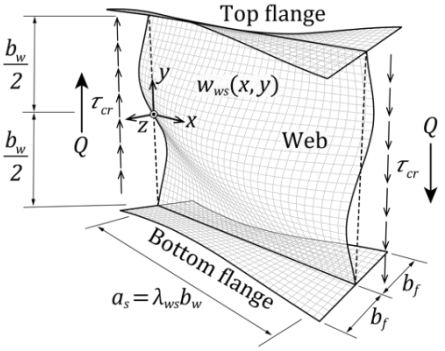

Figure 2. Buckling analysis model under pure shear force

Table 2. Parameters and symbols

λ_{ws}:	Web aspect ratio [-] (= a_s/b_w)	A_w:	Gross area of web [mm²]
a_s:	Length of half-wave along the *x*-axis [mm] (= $\lambda_{ws}\, b_w$)		
c_n,d_n:	Undetermined coefficients	τ_{cr}:	Elastic critical shear buckling stress [N/mm²]

The displacement function along the *y*-axis of the web is approximated using Eqn. (26), which uses the partial sum of Eqn. (25).

$$\begin{aligned} w_{ws} &= \sin\left[\frac{\pi}{a_s}\left(x+\xi b_w \sin\frac{\pi y}{b_w}\right)\right]\cdot\left(c_0+c_1\cos\frac{2\pi y}{b_w}+d_1\cos\frac{\pi y}{b_w}\right) \\ &= \sin\left[\frac{\pi}{a_s}\left(x+\xi b_w \sin\frac{\pi y}{b_w}\right)\right]\cdot\left[\alpha_s\cos\frac{\pi y}{b_w}+\beta_s\left(1+\cos\frac{2\pi y}{b_w}\right)\right] \\ &\left(N=1, \alpha_s=d_1, \beta_s=c_0=c_1\right) \end{aligned} \tag{26}$$

By using the displacement function of the web from Eqn. (26), the displacement function of the flange can be determined. The center of rotation of the flange was assumed to be the junction line between the web and flanges, and it was assumed that the flange deformed out-of-plane while remaining straight and perpendicular to the web. The displacement functions of the top and bottom flanges can be derived by substituting $y = b_w/2$ and $y = -b_w/2$ in Eqn. (27), which was obtained by partially differentiating Eqn. (26) with respect to *y*, which results in Eqns. (28-29).

$$\begin{aligned} &\frac{\partial w_{ws}}{\partial y} = \frac{\pi^2\xi}{a_s}\cos\left[\frac{\pi}{a_s}\left(x+\xi b_w \sin\frac{\pi y}{b_w}\right)\right] \\ &\cdot\cos\frac{\pi y}{b_w}\cdot\left[\alpha_s\cos\frac{\pi y}{b_w}+\beta_s\left(1+\cos\frac{2\pi y}{b_w}\right)\right] \\ &-\frac{\pi}{b_w}\sin\left[\frac{\pi}{a_s}\left(x+\xi b_w \sin\frac{\pi y}{b_w}\right)\right]\cdot\left(\alpha_s\sin\frac{\pi y}{b_w}+2\beta_s\sin\frac{2\pi y}{b_w}\right) \end{aligned} \tag{27}$$

$$\text{Top flange: } w_{fts} = z\cdot\left.\frac{\partial w_w}{\partial y}\right|_{y=\frac{b_w}{2}} = -\frac{\pi\alpha}{b_w}z\sin\frac{\pi\left(x+\xi b_w\right)}{a_s} \tag{28}$$

$$\text{Bottom flange: } w_{fbs} = z\cdot\left.\frac{\partial w_w}{\partial y}\right|_{y=-\frac{b_w}{2}} = \frac{\pi\alpha}{b_w}z\sin\frac{\pi\left(x-\xi b_w\right)}{a_s} \tag{29}$$

2.2.2 Derivation of critical buckling stress formula

In this subsection, a formula for the elastic critical shear buckling load of the I-shaped section members subjected to a pure shear force is derived based on the energy method. In the case where the critical shear buckling stress τ_{cr} acts on the web of the I-shaped member, the critical shear force works on the web only, but does not work on the flanges. Therefore, the increment of external potential energy ΔV_{ws} can be described as shown in Eqn. (30).

$$\Delta V_{ws} = -\int_{-\frac{b_w}{2}}^{\frac{b_w}{2}}\tau_{cr}t_w a_s\frac{\delta_s}{b_w}dy\,, \tag{30}$$

where δ_s is the small displacement of the web caused by the external force. Subsequently, the increments of strain energy for the web, top flange, and bottom flange, denoted as ΔU_{ws}, ΔU_{fts}, and ΔU_{fbs}, can be described by Eqns. (31-33), respectively, by considering the compatibility conditions of the axial displacements caused by the out-of-plane deformation of each plate element.

$$\begin{aligned} \Delta U_{ws} &= \frac{D_w}{2}\int_0^{a_s}\int_{-\frac{b_w}{2}}^{\frac{b_w}{2}}\left[\left(\frac{\partial^2 w_{ws}}{\partial x^2}\right)^2+\left(\frac{\partial^2 w_{ws}}{\partial y^2}\right)^2\right. \\ &+2\nu\left(\frac{\partial^2 w_{ws}}{\partial x^2}\right)\left(\frac{\partial^2 w_{ws}}{\partial y^2}\right)+2(1-\nu)\left.\left(\frac{\partial^2 w_{ws}}{\partial x\partial y}\right)^2\right]dydx \\ &+\int_0^{a_s}\int_{-\frac{b_w}{2}}^{\frac{b_w}{2}}\tau_{cr}t_w\left[\frac{\delta_s}{b_w}-\left(\frac{\partial w_{ws}}{\partial x}\right)\left(\frac{\partial w_{ws}}{\partial y}\right)\right]dydx \end{aligned} \tag{31}$$

$$\begin{aligned} \Delta U_{fts} &= \frac{D_f}{2}\int_0^{a_s}\int_{-b_f}^{b_f}\left[\left(\frac{\partial^2 w_{fts}}{\partial x^2}\right)^2+\left(\frac{\partial^2 w_{fts}}{\partial z^2}\right)^2\right. \\ &+2\nu\left(\frac{\partial^2 w_{fts}}{\partial x^2}\right)\left(\frac{\partial^2 w_{fts}}{\partial z^2}\right)+2(1-\nu)\left.\left(\frac{\partial^2 w_{fts}}{\partial x\partial z}\right)^2\right]dzdx \end{aligned} \tag{32}$$

$$\begin{aligned} \Delta U_{fbs} &= \frac{D_f}{2}\int_0^{a_s}\int_{-b_f}^{b_f}\left[\left(\frac{\partial^2 w_{fbs}}{\partial x^2}\right)^2+\left(\frac{\partial^2 w_{fbs}}{\partial z^2}\right)^2\right. \\ &+2\nu\left(\frac{\partial^2 w_{fbs}}{\partial x^2}\right)\left(\frac{\partial^2 w_{fbs}}{\partial z^2}\right)+2(1-\nu)\left.\left(\frac{\partial^2 w_{fbs}}{\partial x\partial z}\right)^2\right]dzdx \end{aligned} \tag{33}$$

Based on these equations, the total potential energy increment $\Delta\Pi_s$, which is represented by the sum of the strain energy increments and the external potential energy increment, can be obtained as shown in Eqn. (34).

$$\Delta\Pi_s = \Delta U_{ws}+\Delta U_{fts}+\Delta U_{fbs}+\Delta V_{ws} \tag{34}$$

From the stationary condition of the total potential energy, the first variations of Eqn. (34) with respect to the coefficients α_s and β_s yield Eqns. (35-36).

$$\frac{\partial\Delta\Pi_s}{\partial\alpha_s}=0 \tag{35}$$

$$\frac{\partial\Delta\Pi_s}{\partial\beta_s}=0 \tag{36}$$

After performing these differentiations and simplifying them, the buckling condition equation can be obtained as shown in Eqn. (37).

$$\begin{Bmatrix} o_1-o_2\tau_{cr} & o_3-o_4\tau_{cr} \\ o_3-o_4\tau_{cr} & o_5-o_6\tau_{cr} \end{Bmatrix}\begin{Bmatrix}\alpha_s \\ \beta_s\end{Bmatrix}=0 \tag{37}$$

Shear buckling occurred when Eqn. (37) provides a solution other than the trivial solution ($\alpha_s = \beta_s = 0$). Consequently, the determinants of the coefficient matrix on the left-hand side of Eqn. (37) must be zero. Therefore, by calculating the conditions

under which the determinant of the coefficient matrix is zero, Eqn. (38) can be obtained.

$$\left(o_2o_6-o_4^2\right)\tau_{cr}^2-\left(o_1o_6+o_2o_5-2o_3o_4\right)\tau_{cr} +o_1o_5-o_3^2=0 \tag{38}$$

As Eqn. (38) is a quadratic equation with respect to the critical buckling stress τ_{cr}, it should be noted that the minimum positive value of the obtained solutions is the actual critical buckling stress. Consequently, τ_{cr} can be obtained as shown in Eqn. (39).

$$\tau_{cr}=\frac{B_s-\sqrt{B_s^2-4A_sC_s}}{2A_s} \tag{39}$$

$$A_s=o_2o_6-o_4^2 \tag{39a}$$

$$B_s=o_1o_6+o_2o_5-2o_3o_4 \tag{39b}$$

$$C_s=o_1o_5-o_3^2\,, \tag{39c}$$

where o_1–o_6 are functions of λ_{ws} and ξ, as shown in Eqns. (40-45).

$$o_1=\frac{\pi^4D_w}{b_w^2}\left[\left(\frac{5\pi^4\xi^4}{32}+\frac{3\pi^2\xi^2}{8}+\frac{1}{4}\right)\frac{1}{\lambda_{ws}^3} +\left(\frac{13\pi^2\xi^2}{16}+\frac{1}{2}\right)\frac{1}{\lambda_{ws}}+\frac{\lambda_{ws}}{4}\right] +\frac{2\pi^4D_f}{b_w^2}\left[\frac{\pi^2b_f^3}{3b_w^3}\cdot\frac{1}{\lambda_{ws}^3}+2(1-\nu)\frac{b_f}{b_w}\cdot\frac{1}{\lambda_{ws}}\right] \tag{40}$$

$$o_2=\frac{4\pi^2t_w}{3b_w}\cdot\frac{\xi}{\lambda_{ws}} \tag{41}$$

$$o_3=\frac{\pi^4D_w}{b_w^2}\left[\left(\frac{32\pi^3\xi^4}{35}+\frac{32\pi\xi^2}{15}+\frac{4}{3\pi}\right)\frac{1}{\lambda_{ws}^3} +\left(\frac{88\pi\xi^2}{15}+\frac{8}{3\pi}\right)\frac{1}{\lambda_{ws}}+\frac{4\lambda_{ws}}{3\pi}\right] \tag{42}$$

$$o_4=\frac{3\pi^3t_w}{4b_w}\cdot\frac{\xi}{\lambda_{ws}} \tag{43}$$

$$o_5=\frac{\pi^4D_w}{b_w^2}\left[\left(\frac{35\pi^4\xi^4}{64}+\frac{5\pi^2\xi^2}{4}+\frac{3}{4}\right)\frac{1}{\lambda_{ws}^3} +\left(\frac{37\pi^2\xi^2}{8}+2\right)\frac{1}{\lambda_{ws}}+4\lambda_{ws}\right] \tag{44}$$

$$o_6=\frac{64\pi^2t_w}{15b_w}\cdot\frac{\xi}{\lambda_{ws}} \tag{45}$$

The critical shear buckling stress τ_{cr} needs to be minimized with respect to λ_{ws} and ξ in Eqn. (39). In other words, by calculating λ_{ws} and ξ that satisfy Eqn. (46), the critical shear buckling stress τ_{cr} can be obtained.

$$\frac{\partial\tau_{cr}(\lambda_{ws},\xi)}{\partial\lambda_{ws}}=\frac{\partial\tau_{cr}(\lambda_{ws},\xi)}{\partial\xi}=0 \tag{46}$$

The accuracy of the predicted elastic critical buckling stress τ_{cr} that satisfies Eqn. (46) was verified by comparing it with the results of the buckling eigenvalue analysis using the finite element method, as described in the next section.

3 Verification of the accuracy of critical buckling stress formulae using FEM analysis

3.1 Overview of the FEA model

The validity of the proposed critical buckling stresses σ_{cr} and τ_{cr} presented in Section 2 were verified by comparing it with the results of buckling eigenvalue analysis using the finite element method. For verification, a buckling eigenvalue analysis was performed using the FEA program ANSYS (2019R1)[7], with the cross-sectional shapes of the I-shaped members as parameters. The analysis variables under any loading condition areshown in Table 3, and a wide range of cross-sectional shapes based on standard plate thicknesses, which are utilized in practical design, were set as the analysis targets.

Table 3. Analysis variables range (2500 cases)

H [mm]	B [mm]	t_w [mm]	t_f [mm]
400–1500 @50	100–750 @50	6–28	9–50
b_w/t_w	b_f/t_f	H/B	t_f/t_w
48.5–98.9	2.3–13.6	2.0–4.5	1.1–3.1

3.1.1 Under uniform bending

Figure 3 presents an overview of the analytical model. The analytical model consisted of four-node shell elements, for the flanges and web, divided into (b_w/40) × (b_w/40) mm squares based on the examination of solution convergence. The length of the analysis model was set to be 40 times b_w, which was considered infinite to avoid the influence of the boundary conditions at both beam ends on the buckling eigenvalue. The nodes at both ends of the analysis model were connected to the centroid of the cross-section via rigid elements. Centroid positions A and B are pin-supported and pin-roller-

supported, respectively, allowing rotation only around the strong axis at both ends. The nodes along the junction lines of the web and flanges were constrained during out-of-plane deformation. An external force (bending moment, M_{FEM}) was applied as a unit load, as shown in Figure 3, to input a uniform bending moment along the entire length. The critical buckling stress σ_{FEM} is calculated by dividing the eigenvalue obtained from the buckling eigenvalue analysis by the section modulus Z. This value is used to verify the accuracy of σ_{cr} in the previous section. The material properties were set with a Young's modulus E of 205,000 N/mm² and a Poisson's ratio of 0.3.

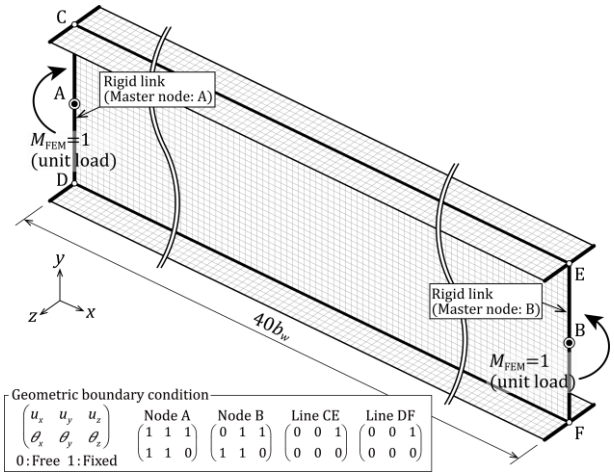

Figure 3. Overview of FEA model and boundary conditions under uniform bending

3.1.2 Under pure shear force

Figure 4 presents an overview of the analytical model. The material properties, element composition, member length, and boundary conditions of the analysis model were identical to those described in the previous section. The external force was applied as a unit load along the x-axis to all nodes along the junction lines of the web and the top and bottom flanges (in opposite directions for the upper and bottom flanges with a load magnitude of 0.5 for the nodes at both ends, considering the tributary area), setting up a pure shear force input to the web. Using the eigenvalue obtained from the buckling eigenvalue analysis, the resultant force Q_{FEM} on one side of the flange (Figure 4) was used to calculate the shear force $Q_{w,FEM}$ acting on the web based on the moment equilibrium around point A. This shear force is then divided by the web cross-sectional area A_w to derive the critical buckling stress τ_{FEM} (Eqn. (47)). This value is used to verify the accuracy of τ_{cr} in the previous section.

$$\tau_{FEM} = \frac{Q_{w,FEM}}{A_w} = \frac{Q_{FEM}}{A_w} \cdot \frac{b_w}{40b_w} \tag{47}$$

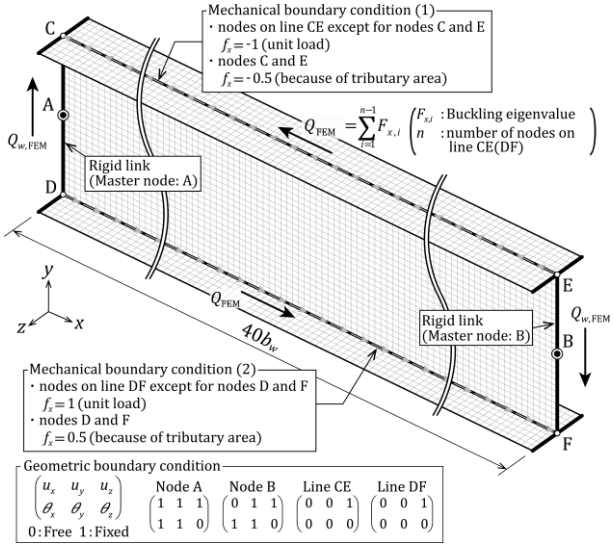

Figure 4. Overview of FEA model and boundary conditions under pure shear force

Verification of the accuracy of the proposed formulae for σ_{cr} and τ_{cr}

Figures 5-6 show the comparison between σ_{cr} and τ_{cr} proposed in Section 2 and the buckling eigenvalue analysis results σ_{FEM} and τ_{FEM} from the previous section. The vertical axis represents the buckling stresses σ_{FEM} and τ_{FEM}, while the horizontal axis represents σ_{cr} and τ_{cr}. Each plot, marked with a circle, corresponds to the analysis cases for the cross-sectional shapes. As indicated in Figures 5-6, σ_{cr} and τ_{cr} accurately predict σ_{FEM} and τ_{FEM}. Specifically, within the range of the cross-sectional shapes in Table 3, the average value of σ_{FEM}/σ_{cr} is 0.973, with a standard deviation of 0.0063 and a maximum error of 4.62%. The average value of τ_{FEM}/τ_{cr} is 0.975, with a standard deviation of 0.0212 and a maximum error of 5.36%, indicating that the proposed formulae have sufficient accuracy for practical use.

4 Conclusions

In this study, we proposed formulae for the elastic critical local buckling stress of infinitely long I-

shaped members, explicitly considering the mutual restraint effects of the flange and web under a uniform bending moment and pure shear force. The effectiveness of these formulae was verified by comparing them with the results of the buckling eigenvalue analysis using the finite element method. For the case of uniform bending moment, the average value of σ_{FEM}/σ_{cr} was 0.973 with a standard deviation of 0.0063 and a maximum error of 4.62%. For the case of pure shear force, the average value of τ_{FEM}/τ_{cr} was 0.975 with a standard deviation of 0.0212 and a maximum error of 5.36%. These results indicate that the proposed formulae accurately predict the buckling eigenvalue analysis results under both loading conditions with sufficient accuracy for practical use.

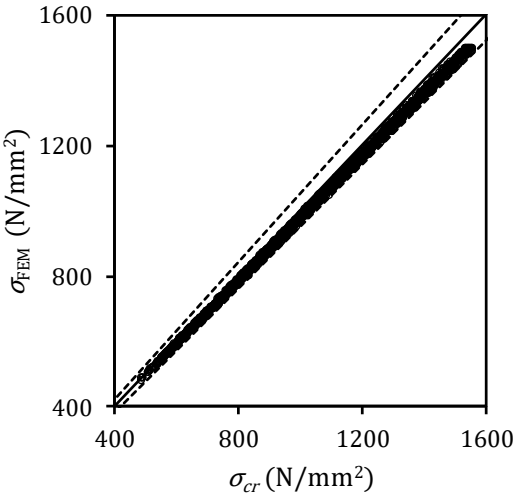

Figure 5. Comparison between σ_{FEM} and σ_{cr}

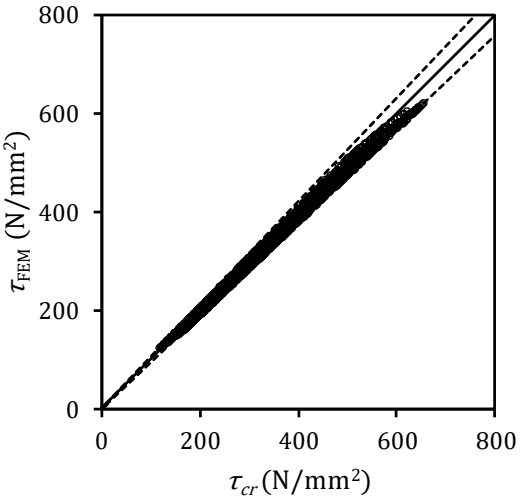

Figure 6. Comparison between τ_{FEM} and τ_{cr}

5 References

[1] Architectural Institute of Japan (AIJ). *AIJ Standard for Allowable Stress Design of Steel Structures*. 2019 (In Japanese).

[2] American Institute of Steel Construction (AISC). *Seismic Provisions for Structural Steel Buildings*. 2016.

[3] CEN Brussels. *EN 1993-1-1 Eurocode3 - design of steel structures Part 1-1 General rules and rules for buildings*. 2005.

[4] Seif M., Schafer BW. Local buckling of structural steel shapes. *Journal of Constructional Steel Research*. 2010;66 (10):1232-1247. doi: 10.1016/j.jcsr.2010.03. 015.

[5] Kato B., Oh YS. Strength and Deformation of I-shaped Steel Members Governed by Local Buckling. *Journal of Structural Engineering*. 1989;35B:351-360(In Japanese).

[6] Matsushita Y., Kato B. Local Buckling Strength and Deformation Capacity of Stainless Steel Members. *Journal of Structural Engineering*. 1993;39B:575-582(In Japanese).

[7] ANSYS, Inc. Ansys Mechanical version 2019 R1. Canonsburg, PA: ANSYS, Inc.; 2019.

Appendix A

The calculation results for the definite integral terms C_1–C_{10} and S_1–S_{10}, which constitute Eqns. (18-23), are shown follows:.

$$C_1 = \int_0^1 \cos 2\pi t^2 dt = 0.2441267 \quad \text{(A1)}$$

$$C_2 = \int_0^1 t^4 \cos 2\pi t^2 dt = 0.01435987 \quad \text{(A2)}$$

$$C_3 = \int_0^1 t^2 \cos 2\pi t^2 dt = -0.01366408 \quad \text{(A3)}$$

$$C_4 = \int_0^1 t^2 \cos \pi t^2 dt = -0.08035010 \quad \text{(A4)}$$

$$C_5 = \int_0^1 t^2 \cos 3\pi t^2 dt = -0.01362173 \quad \text{(A5)}$$

$$C_6 = \int_0^1 \cos \pi t^2 dt = 0.3739828 \quad \text{(A6)}$$

$$C_7 = \int_0^1 \cos 3\pi t^2 dt = 0.2068356 \quad \text{(A7)}$$

$$C_8 = \int_0^1 \cos 4\pi t^2 dt = 0.1752280 \quad \text{(A8)}$$

$$C_9 = \int_0^1 t^4 \cos 4\pi t^2 dt = 0.003917197 \quad \text{(A9)}$$

$$C_{10} = \int_0^1 t^2 \cos 4\pi t^2 dt = -0.005457731 \quad \text{(A10)}$$

$$S_1 = \int_0^1 t^2 \sin 2\pi t^2 dt = -0.06015049 \quad \text{(A11)}$$

$$S_2 = \int_0^1 \sin 2\pi t^2 dt = 0.1717078 \quad \text{(A12)}$$

$$S_3 = \int_0^1 \sin \pi t^2 dt = 0.5048546 \quad \text{(A13)}$$

$$S_4 = \int_0^1 \sin 3\pi t^2 dt = 0.2567635 \quad \text{(A14)}$$

$$S_5 = \int_0^1 t^4 \sin \pi t^2 dt = 0.1207906 \quad \text{(A15)}$$

$$S_6 = \int_0^1 t^4 \sin 3\pi t^2 dt = 0.05088368 \quad \text{(A16)}$$

$$S_7 = \int_0^1 t^2 \sin \pi t^2 dt = 0.2186762 \quad \text{(A17)}$$

$$S_8 = \int_0^1 t^2 \sin 3\pi t^2 dt = 0.06402461 \quad \text{(A18)}$$

$$S_9 = \int_0^1 t^2 \sin 4\pi t^2 dt = -0.03281663 \quad \text{(A19)}$$

$$S_{10} = \int_0^1 \sin 4\pi t^2 dt = 0.1371678 \quad \text{(A20)}$$